

# Rapid Design and Optimization of a Composite Retainer to Support the Energetic Loading of an Expanding Tube Assembly

Richard A. Davis\*

*Pacific Scientific Energetic Materials Company, Hollister, California, 95023*

A novel use of classical laminate theory (CLT) augmented with a subscale test program was utilized to support the immediate need for an optimized composite retainer that could withstand the energetic loading of an Expanding Tube Assembly (XTA). The known bending stiffnesses of a legacy aluminum retainer were used to obtain the number of plies of an equivalent cross-section. The analysis revealed the number of plies and stacking orientation of the new material necessary to yield comparable stiffnesses to the legacy device. Subscale retainers were tested at various thicknesses to optimize and define final cross-section geometry. The optimized cross-section was selected. Additional subscales were tested at the selected thickness for validation.

## Nomenclature

$A$	=	extensional stiffness matrix
$A$	=	area
$D$	=	bending stiffness matrix
$E$	=	elastic modulus
$G$	=	shear modulus
$I$	=	moment of inertia
$i$	=	directional index
$j$	=	directional index
$K$	=	stiffness
$k$	=	ply index
$L$	=	length
$Q$	=	reduced stiffness matrix
$r$	=	radius
$T$	=	transformation matrix
$t$	=	thickness
$z$	=	distance from ply to centroid
$\gamma$	=	shear strain
$\varepsilon$	=	normal strain
$\theta$	=	angle
$\nu$	=	Poisson's ratio
$\sigma$	=	normal stress
$\tau$	=	shear stress
1	=	principal material direction index
2	=	second principal material direction index
3	=	third principal material direction index

---

\* Design Engineer, Advanced Technology - Ordnance, 3601 Union Road, AIAA Professional Member

## I. Introduction

An XTA consists of Mild Detonating Cord (MDC) inside an ovalar-formed rigid tube. The assembly is sealed on both ends by high-energy booster shells that serve as initiation points. The purpose of an XTA is to provide mechanical work for applications such as missile stage separation and canopy jettison.

An XTA functional event starts when the MDC is initiated. The energy it releases causes the formed tube to expand to circular geometry. Figure 1 illustrates an XTA between two flat plates. As the XTA expands, the frangible joint between the plates fractures. Although the pyro event is simple, mathematically characterizing the XTA behavior is a challenge.

A detonation is a shock wave with a rapid exothermic chemical reaction occurring just behind the shock front<sup>†</sup>. Characterizing a detonation event mathematically is very complex. Releating the explosive physics to the equations that govern mechanical behavior further complicates analysis. In explosive mechanics, energetically loaded structures do not behave like materials loaded by typical mechanical sources. In pyro events, materials plastically flow in a manner more like a fluid than a solid. Standard finite element analysis (FEA) approaches fail to accurately simulate the event. An explicit-dynamics method that uses an eulerian-lagrangian approach has proven to accurately correlate simulations with experimental data. This approach captures the nonlinear dynamics of solids, fluids, gases and their interactions<sup>†</sup>. Although simulating an explosive event is possible, preparing the study, correlating to experimental data, performing detailed design, and validating through test can be costly and time consuming. The use of composite structures in explosive systems only adds to the analytical complexity.

Composites have the potential to lower part life-cycle cost for two primary reasons: ease of manufacturing and reduced material waste. Composites allow complex geometries to be manufactured repeatedly from a variety of proven techniques. The ability to repetitively manufacture complex geometries from composite materials can drastically reduce costs compared to machining an equivalent metal part. Material waste is lower for composites than for conventional materials because composites are fabricated close to the final configuration. The fabrication of parts from conventional materials such as aluminum consists of hogging-out (machining) a large blank of material that sometimes weighs as much as seven times the final part weight<sup>2</sup>. Another advantage of using composite materials is structural design efficiency. A major purpose of lamination is to tailor the directional dependence of strength and stiffness of a material to match the loading environment of the structure<sup>2</sup>. The ability to optimize a structure by adding strength only where needed is attractive to designers. With the increased capabilities of composite materials comes increased mathematical involvement. Most load-carrying structures in use are made of isotropic materials, which have been studied for hundreds of years. With composite materials comes material anisotropy. Perhaps the largest challenge of composite design is the increased time spent in the preliminary design phase in overcoming anisotropy.

The complexity of an XTA pyro event and the challenges of composite analysis create a difficult system to evaluate. This paper explains how designers can overcome the analytical challenges of composite pyro structures. It details a tailorable process to convert isotropic material and geometry to an equivalent composite cross-section. The process is augmented by a short test series to optimize and validate the design.

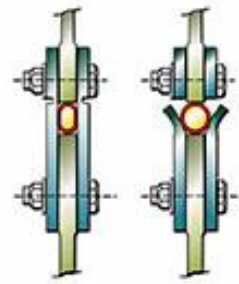


**Figure 1. XTA used in a frangible joint.** *XTAs have seen highly reliable use in the frangible joint application.*

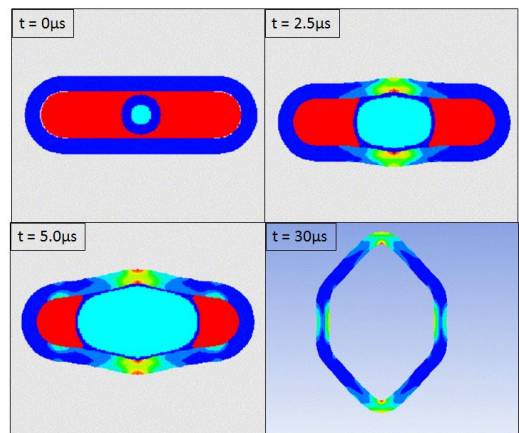


**Figure 2. XTA function.** *XTA simulation illustrates the change in cross-section geometry throughout the energetic event.*

<sup>†</sup> ANSYS Autodyn website reference

## II. Equivalent Cross-section Analysis and Optimization Process

### A. Equivalent cross-section analysis

Obtaining an equivalent cross-section through bending stiffness analysis is simple for isotropic materials. For example, a bronze rod ( $E = 15 \times 10^6$  psi) of 1 inch radius can be equivalently represented by an aluminum rod ( $E = 10 \times 10^6$  psi) of 1.11 inch radius. The mechanical behavior is explained by Eq. (1):

$$K_{bending} = EI_{Bronze} = EI_{Aluminum} \quad (1)$$

where  $K_{bending}$  is the bending stiffness,  $E$  is the elastic modulus, and  $I$  is the moment of inertia. Substituting the known values into Eq. (1) yields an expression in terms of the aluminum rod's radius,  $r$ :

$$\left(15 * 10^6 \frac{lb}{in^2}\right) \left(\frac{\pi}{4} 1^4\right) = \left(10 * 10^6 \frac{lb}{in^2}\right) \left(\frac{\pi}{4} r_{Aluminum}^4\right) \quad (2)$$

Solving Eq. (2) for  $r_{Aluminum}$  yields a value of 1.11 inches. Thus, a bronze rod of a 1 inch radius can be replaced by an aluminum rod of 1.11 inch radius to yield a member with similar bending performance. Through simple algebraic manipulation, an equivalent cross-section can be found. The same analysis is not as simple when converting an isotropic member to a composite equivalent.

Each layer in a composite laminate can have a significant strength bias in a particular direction. When layers of composite material are oriented in various directions, each layer has an impact on the macro-mechanical characteristics of the laminate. Thus, an analytical method that examines each layer's impact on the mechanical characteristics is needed. Before this method is discussed, a brief discussion of failure modes is needed.

The objective in finding an equivalent composite section starts by determining the possible failure modes of the member to be replaced. If the member fails in axial tension or compression then the extensional stiffnesses are examined. If the member fails in bending then the bending stiffnesses are examined. Often, the failure is a result of a combined load in which case both extensional and bending stiffnesses should be considered. Both extensional and bending stiffnesses are a function of elastic moduli and ply orientation. The stress level carried by each lamina in a laminate depends on its elastic moduli. This may cause large stress gradients between laminae which are oriented at considerably large angles to each other. If the stress gradients are close to a limit value, fracture may occur<sup>3</sup>.

Figure 3 illustrates the analysis portion of the process, which transforms material and laminate stacking characteristics into useful macro-mechanical stiffness matrices.

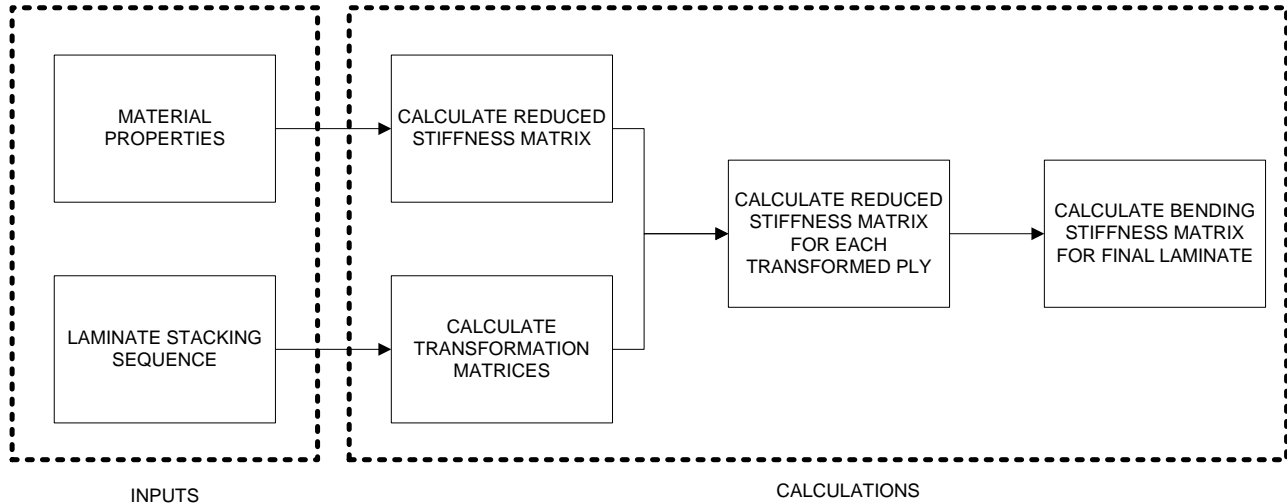


Figure 3. Laminate bending stiffness calculation process.

Understanding the stiffness equations requires understanding the composite stress-strain relationships. For a specially orthotropic lamina, whose principal material axes are aligned with the natural body axes, the stress-strain

relations are specified by Eq. (3)<sup>2</sup>. This relation is for a single ply. Note that the  $\sigma_3$ ,  $\tau_{23}$ ,  $\tau_{13}$ ,  $\gamma_{23}$ , and  $\gamma_{31}$  elements have been omitted from the matrix. These elements are equal to zero due to the specially orthotropic assumption.

$$\begin{bmatrix} \sigma_1 \\ \sigma_2 \\ \tau_{12} \end{bmatrix} = \begin{bmatrix} \frac{E_1}{(1-\nu_{12}\nu_{21})} & \frac{\nu_{12}E_2}{(1-\nu_{12}\nu_{21})} & 0 \\ \frac{\nu_{21}E_1}{(1-\nu_{12}\nu_{21})} & \frac{E_2}{(1-\nu_{12}\nu_{21})} & 0 \\ 0 & 0 & G_{12} \end{bmatrix} \begin{bmatrix} \varepsilon_1 \\ \varepsilon_2 \\ \gamma_{12} \end{bmatrix} \quad (3)$$

where  $\sigma$  is normal stress,  $\tau$  is shear stress,  $\varepsilon$  is normal strain,  $\gamma$  is shear strain,  $\nu$  is Poisson's ratio, and  $G$  is the shear modulus.

The 3X3 matrix in Eq. (3) is the reduced stiffness matrix. This matrix is signified by  $[Q]$ . The reduced stiffness matrix relates stresses and strains in the principle directions of the material. To define the material response in directions other than these coordinates, transformation relations for the material stiffnesses are needed<sup>4</sup>.

The transformation matrix for each ply is the following:

$$[T_\theta] = \begin{bmatrix} \cos^2 \theta & \sin^2 \theta & 2 \sin \theta \cos \theta \\ \sin^2 \theta & \cos^2 \theta & -2 \sin \theta \cos \theta \\ -\sin \theta \cos \theta & \sin \theta \cos \theta & \cos^2 \theta - \sin^2 \theta \end{bmatrix} \quad (4)$$

where  $[T]$  is the transformation matrix and  $\theta$  is the angle of the ply under consideration with respect to the principal material axis.

From  $[Q]$  and  $[T]$  the reduced stiffness matrix for each ply can be calculated from the following equation:

$$[\bar{Q}] = [T]^{-1} [Q] [T]^T \quad (5)$$

where the bar over the reduced stiffness matrix signifies the transformed condition.

From Eq. (5), the matrix describing extensional stiffness,  $[A_{ij}]$ , and bending stiffness,  $[D_{ij}]$ , can be determined from the following equations:

$$[A_{ij}] = \sum_{k=1}^N [\bar{Q}_{ij}]_k (t_k) \quad (6)$$

$$[D_{ij}] = \sum_{k=1}^N [\bar{Q}_{ij}]_k \left( t_k \bar{z}_k^2 + \frac{t_k^3}{12} \right) \quad (7)$$

where  $t$  is the ply thickness and  $z_k$  is the distance to the centroid of the  $k^{\text{th}}$  ply. The terms of the stiffness matrices above can be compared to the isotropic material stiffness,  $K$ , to determine if cross-sectional equivalency is reached.

The units of extensional stiffness are pound/inch, which can be compared directly to the extensional stiffness of an isotropic member, which is:

$$K_{\text{extensional}} = \frac{AE}{L} \quad (8)$$

The units for bending stiffness are pound-inch but those for isotropic bending stiffness are pound-inch-inch. The two values cannot be compared directly. The reason for this difference is the bending stiffness matrix assumes a unit cross-section where the isotropic equation does not. The isotropic value can be calculated as if it were of unit length to obtain a direct relationship.

Examining the extensional and bending stiffness matrix elements on the main diagonal reveals properties in each of the three principal material directions. These values can be compared with the isotropic properties to determine if cross-section equivalency is obtained.

### B. Optimization through test

There are three objectives of the test process: optimize cross-sectional geometry, establish safety factor (margin), and validate the selection. The optimization process is illustrated in Fig. 4.

The process starts by testing the cross-section determined by stiffness analysis. If the result is a success, the stiffness is decreased i.e. less plies, different stacking geometry. The test is repeated until a failure occurs. Once a failure occurs, the previous test configuration is selected with additional safety factor. The selection is validated through a test series.

If the configuration determined by analysis results in a test failure, the section stiffness of the next unit is increased. This process is repeated until a success is reached. This configuration is selected with safety factor added. The selection is validated through a test series.

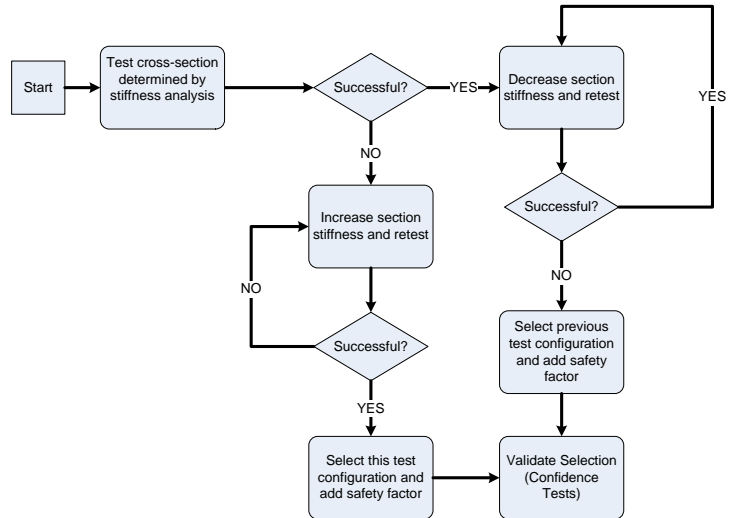


**Figure 4. Optimization test process.** The cross-sectional geometry determined from analysis serves as the starting point for optimization testing. Through a number of test iterations, a final selection is made and validated.

## III. Analysis and Test Results of a Composite Retainer Loaded by an XTA

### A. Analysis

The aluminum legacy device was energetically loaded and supported as shown in Fig. 5. The purpose of the retainer is to provide the bending stiffness necessary to support the XTA against the substrate it is intended to fracture. Once the substrate is broken, the retainer will immediately be unloaded. If the retainer fails to withstand the XTA's loads in bending, then the system will fail. The failure point will likely be at the boundary condition where the retainer is supported. At this location, the moment arm is the largest and the retainer will see the highest stresses when loaded. When the XTA is functioned the retainer will bend like a simple cantilever beam with a point load on the end. The objective of the analysis will be to replicate the critical section stiffness shown in Fig. 5 into the composite equivalent.

Using Eq. (1), the critical section stiffness of the legacy device was found to be approximately 1600 lb-in<sup>2</sup>. Using Eqs. (3), (4), (5), and (7), it was found that approximately 18 plies of composite material oriented in a semi-isotropic stacking pattern would yield

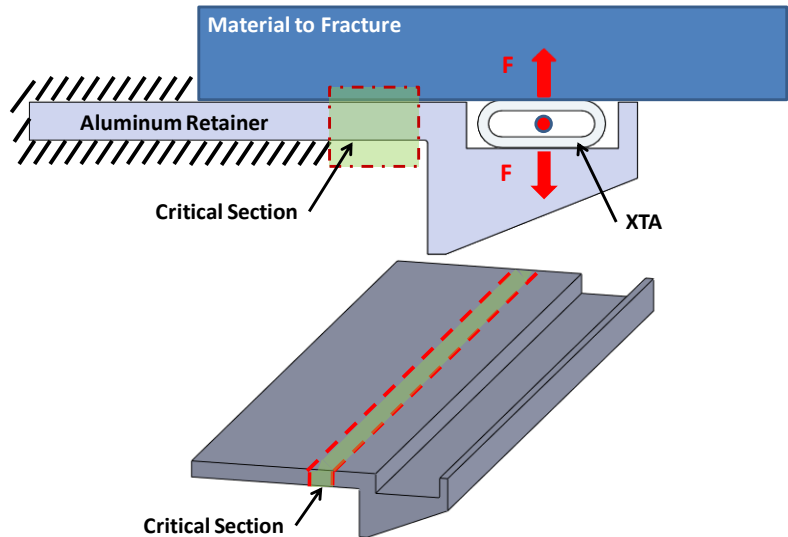


**Figure 5. System load diagram.** The device is cantilevered off a fixed end support. As the XTA expands, the force it imparts on the retainer and material substrate causes the retainer to bend in the region labeled "Critical Section."

approximately equivalent bending performance. The 18-ply equivalent composite part would be the starting point of the test and optimization phase.

## B. Test Results

Optimization tests were conducted using the process shown in Fig. 4. Table 1 shows successive XTA firings and the retainer decisions made.

**Table 1. Functional test results and decisions made.**

Test Number	Ply	Critical Section Stiffness	Fracture Result	Decision
1	18	1600 lb-in <sup>2</sup>	Complete fracture	Decrease stiffness
2	16	1100 lb-in <sup>2</sup>	Complete fracture	Decrease stiffness
3	14	1000 lb-in <sup>2</sup>	Complete fracture	Decrease stiffness
4	12	800 lb-in <sup>2</sup>	Complete fracture	Decrease stiffness
5	10	700 lb-in <sup>2</sup>	Partial fracture	Select 14 ply configuration for validation firings
6	14	1000 lb-in <sup>2</sup>	Complete fracture	Validation
7	14	1000 lb-in <sup>2</sup>	Complete fracture	Validation
8	14	1000 lb-in <sup>2</sup>	Complete fracture	Validation
9	14	1000 lb-in <sup>2</sup>	Complete fracture	Validation
10	14	1000 lb-in <sup>2</sup>	Complete fracture	Validation
11	14	1000 lb-in <sup>2</sup>	Complete fracture	Validation
12	14	1000 lb-in <sup>2</sup>	Complete fracture	Validation
13	14	1000 lb-in <sup>2</sup>	Complete fracture	Validation
14	14	1000 lb-in <sup>2</sup>	Complete fracture	Validation
15	14	1000 lb-in <sup>2</sup>	Complete fracture	Validation
16	14	1000 lb-in <sup>2</sup>	Complete fracture	Validation

Although the 12 ply configuration was the last configuration to fully fracture the material substrate, we are unable to determine if this configuration is marginal. Therefore, the 14 ply configuration was chosen for validation. The 14 ply configuration has nearly 25% higher critical section stiffness than the 12 ply configuration. The data shows the legacy aluminum device may have been overdesigned because the composite retainer selected had nearly 60% less stiffness than the legacy aluminum retainer.

The prescribed testing plan allowed the composite retainer cross-sectional geometry to be optimized and validated. The optimization tests saved approximately 20% in material costs over the 18 ply configuration.

## IV. Conclusion

Energetic load-carrying structures can be a challenge to characterize. Furthermore, adding the anisotropy of composite materials to any analysis makes the detailed design phase even more demanding. Utilizing CLT analysis and the optimization test process suggested can be great way to minimize the time spent in preliminary design. The process is simple for engineers that do not have a strong background in composite theory to soundly design load carrying structures.

The process described in the sections above can be a powerful technique to rapidly design and optimize a composite system. The process is not recommended to replace a qualification or verification activity. The purpose of the analysis and test methods is to quickly move into more rigorous qualification test activities. The process is only a starting point and is meant to be tailored to meet the intended system's requirements..

## References

- <sup>1</sup>Cooper, P. W., *Explosives Engineering*, Wiley-VCH, New York, 1996, Chap 14.
- <sup>2</sup>Jones, R. M. (1<sup>st</sup> ed.), *Mechanics of Composite Materials*, Hemisphere Publishing Corporation, New York, 1975, Chaps 1 and 2.
- <sup>3</sup>Altenbach, H., Altenbach, J. W., Kissing, W., *Mechanics of Composite Structural Elements*, Springer-Verlag, Berlin Heidelberg New York, 2004, pp. 183.

<sup>4</sup> “Department of Defense Handbook – Composite Materials Handbook (Vol. 3),” *MIL-HDBK-17-3F Polymer Matrix Composites, Material Usage, Design, and Analysis*, Washington, DC, 2002, pp. 233-234.